

# $N^*$ Form Factors based on a Covariant Quark Model<sup>†</sup>

G. Ramalho

Published date: June 4, 2018

**Abstract** We discuss the results of the covariant spectator quark model for the several  $\gamma^*N \rightarrow N^*$  transitions, where  $N$  is the nucleon and  $N^*$  a nucleon excitation. More specifically, we present predictions for the form factors and transition amplitudes associated with the resonances  $N(1440)1/2^+$ ,  $N(1535)1/2^-$ ,  $N(1520)3/2^-$ ,  $\Delta(1620)1/2^-$  and  $N(1650)1/2^-$ . The estimates based on valence quark degrees of freedom are compared with the available data, particularly with the recent Jefferson Lab data at low and large momentum transfer ( $Q^2$ ). In general the estimates are in good agreement with the empirical data for  $Q^2 > 2 \text{ GeV}^2$ , with a few exceptions. The results are discussed in terms of the role of the valence quarks and the meson cloud excitations for the different resonances  $N^*$ . We also review our results for the resonance  $\Delta(1232)3/2^+$  and discuss the relevance of the pion cloud component for the magnetic dipole form factor and the electric and Coulomb quadrupole form factors.

**Keywords** Nucleon excitations · Electromagnetic structure · Valence quarks · Meson cloud

---

<sup>†</sup> This is a post-peer-review, pre-copyedit version of an article published in *Few-Body Syst*, **59** (2018). The final authenticated version is available online at: <http://doi.org/10.1007/s00601-018-1412-9>.

G. Ramalho  
Laboratório de Física Teórica e Computacional – LFTC,  
Universidade Cruzeiro do Sul, 01506-000, São Paulo, SP, Brazil  
Tel.: +55 11 3385-3004  
E-mail: gilberto.ramalho@cruzeirosul.edu.br

## 1 Introduction

Modern accelerators, such as MAMI, MIT-Bates and Jefferson Lab (JLab) provide nowadays important information about the electromagnetic structure of the nucleon ( $N$ ) and nucleon excitation ( $N^*$ ) up to masses of 2 GeV [1, 2, 3, 4, 5]. The data associated to the  $\gamma^*N \rightarrow N^*$  transition, for the photon momentum  $q$  can be represented in terms of structure functions, transition form factors or helicity amplitudes, dependent on the transition momentum square  $q^2$ , or from  $Q^2 = -q^2$ . In the recent years data associated with several resonances  $N^*$  have been collected at JLab up to  $Q^2 = 6 \text{ GeV}^2$ . With the JLab-12 GeV upgrade, we expect to achieve in a near future  $Q^2 \simeq 12 \text{ GeV}^2$  [1].

To interpret the recent data at the range  $Q^2 = 2\text{--}6 \text{ GeV}^2$  and above, it is necessary to develop theoretical models based on relativity. Preferable are models based on the dominant degrees of freedom at large  $Q^2$ , the valence quarks. However, models that take into account the degrees of freedom associated with the quark-antiquark/meson states may be also appropriated to understand the transition between the low and large  $Q^2$  regimes. These models can be used to make predictions for transition form factors at large  $Q^2$ , and may also be used to guide future experiments as the ones projected to the JLab-12 GeV upgrade [1, 3, 6, 7, 8].

Different frameworks have been used in the study of the  $\gamma^*N \rightarrow N^*$  transitions, such as, quark models, effective chiral perturbation theories, dynamical coupled-channel models, Dyson-Schwinger equations, large  $N_c$  limit, QCD sum rules, perturbative QCD and lattice QCD simulations, among others [1, 2]. As mentioned, frameworks based on valence quarks are particularly useful at large  $Q^2$ , since those degrees of freedom are expected to be dominant.

In the present work we discuss mainly results based on the covariant spectator quark model. The covariant spectator quark model is a model based on constituent quarks where the quark electromagnetic is parametrized in order to describe the nucleon electromagnetic structure [6]. The wave functions of the baryons are ruled by the  $SU(6) \otimes O(3)$  symmetry, with radial wave functions determined phenomenologically with the assistance of empirical data, lattice data or estimates of the quark core contributions [6, 7, 8, 9, 10, 11]. One can then use parametrizations of a few resonances  $N^*$  to make predictions for other states based on the symmetries. In this work we present a few examples. The model is covariant by construction and therefore can be used at very large  $Q^2$ . In some cases the model can be extended with the inclusion of effective descriptions of the meson cloud effects, that can be significant at small  $Q^2$  [1, 2, 3, 7, 8]. In Sect. 5 this methodology is illustrated for the case of the  $\gamma^*N \rightarrow \Delta(1232)$  transition. The details about the covariant spectator quark model are discussed in the next section (Sect. 2).

In the following sections, we discuss the results for several  $\gamma^*N \rightarrow N^*$  form factors. We start with our recent results for the  $N(1535)1/2^-$  and  $N(1520)3/2^-$  resonances in the context of the semirelativistic approximation (Sect. 3). Next, we discuss briefly the results for the  $N(1440)1/2^+$  based on the covariant spectator quark model and also an estimate of the valence quark contributions

based on holographic methods (Sect. 4). In Sect. 5, we review the covariant spectator quark model results for the  $\Delta(1232)3/2^+$  and discuss also some recent results for the quadrupole form factors in the light of Siegert's theorem. We finish our presentation of results with the estimates of the negative parity states from the  $[70, 1^-]$  supermultiplet, combining the covariant spectator quark model with the single quark transition model, for the cases  $N(1650)1/2^-$  and  $\Delta(1620)1/2^-$  (Sect. 6). At the end, we summarize the results and conclusions associated with the resonances  $N^*$  discussed in the present work (Sect. 7).

## 2 Covariant Spectator Quark Model

The covariant spectator quark model is based on the covariant spectator theory [6, 12, 13]. The model treats the baryons, including the nucleon and the nucleon excitations, as three-quark systems [6, 14, 15]. The baryon wave functions are expressed in terms of the quarks states, according with the  $SU(6) \otimes O(3)$  symmetry group [16, 17]. In the spectator theory the baryon can be regarded as an off-mass-shell quark free to couple with the photon fields and two spectator on-mass-shell quarks [6, 9, 14, 18, 19]. One can integrate over the quark-pair degrees of freedom and reduce the baryon a quark-diquark system, where the diquark represents an on-shell spectator particle with an effective mass  $m_D$  [6, 9, 14]. At the end, we obtain an effective quark-diquark wave function, free of singularities which include the quark confinement implicitly [6, 9, 13, 14, 20, 21].

In the covariant spectator quark model the electromagnetic interaction is described by the photon coupling with the constituent quarks in relativistic impulse approximation. The structure of the constituent quarks is represented by the quark structure form factors which encode effectively the gluon and quark-antiquark substructure of those quarks [6, 9]. In the  $SU(2)$  flavor sector, one uses the form [6]

$$j_q^\mu = \left( \frac{1}{6}f_{1+} + \frac{1}{2}f_{1-}\tau_3 \right) \gamma^\mu + \left( \frac{1}{6}f_{2+} + \frac{1}{2}f_{2-}\tau_3 \right) \frac{i\sigma^{\mu\nu}q_\nu}{2M_N}, \quad (1)$$

where  $M_N$  is the nucleon mass and  $f_{i\pm}$  ( $i = 1, 2$ ) are the isoscalar/isovector components of the Dirac ( $i = 1$ ) and Pauli ( $i = 2$ ) quark form factors. In Eq. (1),  $\tau_3$  is the Pauli operator and acts on the isospin states of the baryons. For more details, check Refs. [6, 9, 18, 19]. The quark current (1) can be generalized to the  $SU(3)$  sector [9, 18, 22] and to the axial-vector case [23].

For convenience, we label the nucleon resonance  $N^*$  by  $R$ . When the nucleon wave function ( $\Psi_N$ ) and the resonance wave function ( $\Psi_R$ ) are both expressed in terms of the single quark and quark-pair states, the transition current in impulse approximation can be written as [6, 9, 14]

$$J^\mu = 3 \sum_\Gamma \int_k \bar{\Psi}_R(P_R, k) j_q^\mu \Psi_N(P_N, k), \quad (2)$$

where  $P_R$ ,  $P_N$ , and  $k$  are the resonance, the nucleon, and the diquark momenta, respectively. In the previous equation the index  $\Gamma$  labels the intermediate

diquark polarization states, the factor 3 takes account of the contributions from the other quark pairs by the symmetry, and the integration symbol represents the covariant integration over the diquark on-mass-shell momentum. In the study of the inelastic transitions we use the Landau prescription to ensure the current conservation [10, 24, 25, 26].

Using Eq. (2), we can express the transition current in terms of the quark electromagnetic form factors  $f_{i\pm}$  ( $i = 1, 2$ ) and the radial wave functions  $\psi_N$  and  $\psi_R$  [6, 10, 25, 26]. The radial wave functions  $\psi_B(P, k)$ , with  $B = N, R$ , are scalar functions that depend on the baryon ( $P$ ) and diquark ( $k$ ) momenta, and parametrize the momentum distributions of the quark-diquark systems. Since the baryon and the diquark are both on-mass-shell the dependence on the momenta can be expressed in terms of the dimensionless variable  $\chi = \frac{(M_B - m_D)^2 - (P - k)^2}{M_B m_D}$ , where  $M_B$  and  $m_D$  are the baryon and the diquark masses, respectively [6, 9].

The quark electromagnetic form factors  $f_{i\pm}$  are parametrized according to a vector meson dominance mechanism [6, 9, 11, 27]. Taking advantage of the quark form factor structure based on vector meson dominance, the model has been extended to the lattice QCD regime (heavy pions and no meson cloud) [9, 11, 18, 22, 27], to the nuclear medium [19] and to the timelike regime ( $Q^2 < 0$ ) [28, 29, 30]. In the generalization to those regimes we use the representation of the radial wave functions  $\psi_R$  in terms of the diquark mass ( $m_D$ ) and baryon mass ( $M_B$ ) [11, 27].

The covariant spectator quark model was originally developed for the nucleon electromagnetic structure [6]. In this first study it was shown that the electromagnetic structure of the nucleon can be described based on a calibration of quark electromagnetic form factors  $f_{i\pm}$  defined by Eq. (1) and an appropriated form for the radial wave function  $\psi_N(P, k)$ . The parametrization from Ref. [6] for the quark current and radial wave function have been used in all subsequent calculations of the  $\gamma^* N \rightarrow N^*$  transition form factors.

The previous description of the covariant spectator quark model takes into account only the effects associated with the valence quark degrees of freedom. There are however some processes, such as the meson exchanged between the different quarks inside the baryon, which cannot be reduced to processes associated with the dressing of a single quark. Those processes can be regarded as a consequence of the meson exchanged between the different quarks inside the baryon, and can be classified as meson cloud corrections to the hadronic reactions [18, 26, 28, 31, 32]. As mentioned the meson cloud effects can be very significant at small  $Q^2$ .

The study of the role of the meson cloud effects on the  $\gamma^* N \rightarrow N^*$  transition can be done also in the context of the dynamical coupled-channel reaction models [2, 33, 34]. Those models use baryon-meson states to describe the photo- and electro-production of mesons by nucleons, taking into account the meson dressing of propagators and vertices. Once determined the meson couplings by fits to the data, the framework can be used to extract indirectly the effect of the bare core contribution to the data, removing the effect of the meson-baryon

dressings of propagators and vertices. Those estimates of the bare core can be very useful to test the limits of models based on valence quarks, as discussed in Sect. 5, for the case of the  $\Delta(1232)$ . Examples of dynamical coupled-channel reaction models are the Sato-Lee [35], the DMT [36] and the EBAC/Argonne-Osaka models [33, 34, 37].

The model generalized to the  $SU(3)$ -flavor sector have been used in the calculation of octet and decuplet form factors [9, 18, 22, 31, 32, 38, 39, 40, 41], and other transition form factors in the spacelike region ( $Q^2 > 0$ ) [10, 42, 43]. The model also has been used in studies of the electromagnetic structure of resonances  $N^*$  in the timelike region ( $Q^2 < 0$ ) [28, 29, 30]. Applications of the model to the axial and deep inelastic structure of the nucleon can be found in Refs. [6, 14, 15, 23].

In the following sections we discuss the results from the covariant spectator quark model for the electromagnetic structure of resonances  $\Delta(1232)3/2^+$ ,  $N(1440)1/2^+$ ,  $N(1535)1/2^-$ ,  $N(1520)3/2^-$ ,  $\Delta(1620)1/2^-$  and  $N(1650)1/2^-$ .

### 3 $N(1535)1/2^-$ and $N(1520)3/2^-$

We now discuss the negative parity states  $N(1535)$  and  $N(1520)$ . In this study, we use previous calculations based on the covariant spectator quark model [25, 26, 28], combined with the semirelativistic approximation, described below.

#### 3.1 Semirelativistic approximation

As mentioned, the information about the  $\gamma^*N \rightarrow N^*$  transitions can be characterized by transition form factors dependent on the invariant  $Q^2$ . For the discussion of the kinematics, it is however convenient to choose a specific frame. In the following discussion, we use  $|\mathbf{q}|$  to represent the photon three-momentum at the resonance  $R$  rest frame.

The description of the  $\gamma^*N \rightarrow N^*$  transition is simplified in a nonrelativistic framework, because in that case we do not need to take into account the energy component. In these conditions, the orthogonality between states is defined when  $|\mathbf{q}| = 0$ , and both particles are at rest ( $E_R \approx E_N \approx M_N$ ). As a consequence, the transition form factors are independent of the resonance mass [24].

In a relativistic framework the discussion become more intricate because there are ambiguities related with the relativistic generalization of the states. One of the problems is the definition the orthogonality between states, since the two states cannot be at rest in the same frame, unless  $M_R = M_N$ . At  $Q^2 = 0$  one can write  $|\mathbf{q}| = \frac{M_R^2 - M_N^2}{2M_R}$ , therefore, one has  $|\mathbf{q}| = 0$ , only in the limit  $M_R = M_N$ . These ambiguities difficult the calculation of transition amplitudes and helicity amplitudes in some cases when  $M_R \neq M_N$  [25, 26].

In the semirelativistic approximation, we start by considering the approximation  $M_R = M_N$  in the calculation of the elementary form factors, defined

precisely in the following sections. In the next step we use those results to calculate the multipole form factors and helicity amplitudes, which are defined for  $M_R \neq M_N$ , and compare the results with the measured data [24]. An important aspect about the semirelativistic approximation is the way the radial wave functions  $\psi_R$  are defined. We use a form for  $\psi_R$  that allows us to obtain parameter free results for the transition form factors and the helicity amplitudes, based on a relation between  $\psi_R$  and  $\psi_N$ .

With the semirelativistic approximation one tries then to achieve two goals. On the one hand, we want to keep the nice analytic proprieties of the form factors which are spoiled in the relativistic generalization of the wave functions in the case  $M_R \neq M_N$ . On the other hand, we want to describe the experimental helicity amplitudes, which are defined only in the case  $M_R \neq M_N$  [24].

### Notation

Before discussing the  $N(1535)$  and  $N(1520)$  cases it is convenient to introduce some general notation.

To represent the transition form factors we use the symmetric ( $S$ ) and anti-symmetric ( $A$ ) combination of quark currents, which are expressed as a combination of quark form factors [6, 18, 19] ( $i = 1, 2$ ):

$$j_i^S = \frac{1}{6}f_{i+} + \frac{1}{2}f_{i-}\tau_3, \quad j_i^A = \frac{1}{6}f_{i+} - \frac{1}{6}f_{i-}\tau_3. \quad (3)$$

It is also convenient to consider the following overlap integral

$$\mathcal{I}_R(Q^2) = \int_k \frac{k_z}{|\mathbf{k}|} \psi_R(P_R, k) \psi_N(P_N, k), \quad (4)$$

where  $P_R$  and  $P_N$  are the momentum of the resonance and nucleon respectively. For simplicity, we expressed the integral (4) at the resonance rest frame, but it can be generalized to an arbitrary frame [24, 25, 26].

An important characteristic of the semirelativistic approximation is that we assume that the radial wave functions of the resonances can be defined in the rest frame by the nucleon wave function,  $\psi_R \equiv \psi_N$ . As a consequence of this assumption, one has [24]

$$\mathcal{I}_R \propto |\mathbf{q}|, \quad (5)$$

in the limit  $M_R \rightarrow M_N$ .

The previous equation implies that the resonance  $R$  and the nucleon are orthogonal states, since in the limit  $Q^2 = 0$ , one has  $|\mathbf{q}| = 0$ . Another consequence of Eq. (5) is that the final results are independent of the radial structure of the resonance  $R$  and depend only on the parametrization of  $\psi_N$ . As a consequence, the estimates based on the semirelativistic approximation have no free parameters, apart the parameters used on  $\psi_N$ , and then provide true predictions for the transition form factors and helicity amplitudes.

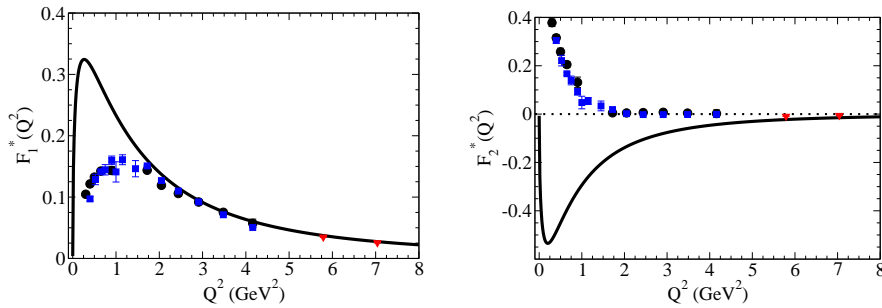


**Fig. 1**  $\gamma^* N \rightarrow N(1535)$  transition form factors. Data from MAID [4], CLAS [44] and JLab/Hall C [45].

In the following, we implement the semirelativistic limit replacing the dependence on  $M_R$  and  $M_N$  by the  $M$ , where  $M \equiv \frac{1}{2}(M_N + M_R)$ . Using this notation, we can write  $|\mathbf{q}| = Q\sqrt{1 + \tau}$ , with  $\tau = \frac{Q^2}{4M^2}$ .

### 3.2 $N(1535)1/2^-$

The  $\gamma^* N \rightarrow N(1535)$  transition current can be expressed using units of elementary charge ( $e$ ), in the form

$$J^\mu = \bar{u}_R \left[ F_1^* \left( \gamma^\mu - \frac{\not{q}q^\mu}{q^2} \right) + F_2^* \frac{i\sigma^{\mu\nu} q_\nu}{M_R + M_N} \right] \gamma_5 u_N, \quad (6)$$

where  $u_R$  and  $u_N$  are the resonance and nucleon spinors, respectively. Equation (6) defines the elementary form factors, Dirac ( $F_1^*$ ) and Pauli ( $F_2^*$ ) [1, 24, 25].

In the semirelativistic limit, we obtain the following results [24]:

$$F_1^* = \frac{1}{2}(3j_1^S + j_1^A)\mathcal{I}_R, \quad F_2^* = -\frac{1}{2}(3j_2^S - j_2^A)\mathcal{I}_R. \quad (7)$$

The numerical results for the form factors are presented in Fig. 1, in comparison with the data from Refs. [4, 44, 45].

Both form factors vanish at  $Q^2 = 0$  as a consequence of the relation  $F_i^*(Q^2) \propto |\mathbf{q}|$ . For the Dirac form factor we obtain a good description of the data for  $Q^2 > 2 \text{ GeV}^2$ . As for  $F_2^*$  the model fails to describe the sign of the data. We can notice in addition that in the  $Q^2 > 2 \text{ GeV}^2$  region the experimental value of the Pauli form factor is compatible with zero ( $F_2^* \simeq 0$ ).

The failure of the semirelativistic approximation for the Dirac form factor below  $2 \text{ GeV}^2$ , and for the Pauli form factor can be interpreted as a consequence of the omission of the meson cloud effects [24]. Our results for both form factors compare well with a previous estimate of the bare core contributions based on the EBAC coupled-channel dynamical model [37]. Our present results can be tested in a near future by new estimates based on the Argonne-Osaka model [46].

The discussion about the implications of the result  $F_2^* \simeq 0$ , and the possible physical interpretations are presented at the end of the section.

As a consequence of the model results for  $F_2^*$ , the model estimates are not comparable with the experimental helicity amplitudes, except in some specific limits. A more detailed discussion can be found in Ref. [24].

### 3.3 $N(1520)1/2^-$

The  $\gamma^* N \rightarrow N(1520)$  transition current can be expressed, in units  $e$ , as [26, 28]:

$$J^\mu = \bar{u}_\alpha [G_1 q^\alpha \gamma^\mu + G_2 q^\alpha P^\mu + G_3 q^\alpha q^\mu + \dots] u_N \quad (8)$$

where  $u_\alpha$  is the Rarita-Schwinger of the  $R$  state,  $u_N$  is the nucleon spinor,  $P = \frac{1}{2}(P_R + P_N)$ , and the dots indicate gauge terms that are not relevant to the present discussion. The functions  $G_i$  ( $i = 1, 2, 3$ ) are the elementary form factors of the transition.

The results for the elementary form factors in the semirelativistic approximation are [24]:

$$G_1 = -\frac{3}{2\sqrt{2}} \left[ \left( j_1^A + \frac{1}{3} j_1^S \right) + \left( j_2^A + \frac{1}{3} j_2^S \right) \right] \frac{\mathcal{I}_R}{|\mathbf{q}|} \quad (9)$$

$$G_2 = +\frac{3}{2\sqrt{2}M} \left[ j_2^A + \frac{1}{3} \frac{1-3\tau}{1+\tau} j_2^S + \frac{4}{3} j_1^S \right] \frac{\mathcal{I}_R}{|\mathbf{q}|} \quad (10)$$

$$G_3 = 0, \quad (11)$$

where  $\tau = \frac{Q^2}{(M_R + M_N)^2} \equiv \frac{Q^2}{4M^2}$ .

For the purpose of the discussion, we note that  $G_1$  and  $G_2$  are proportional to  $\frac{\mathcal{I}_R}{|\mathbf{q}|}$  and are therefore well defined at the photon point, according with Eq. (5).

The previous results for the elementary  $G_i$  ( $i = 1, 2, 3$ ) can be used to calculate the multipole form factors  $G_M$ ,  $G_E$  and  $G_C$  as well as the amplitudes  $A_{1/2}$ ,  $A_{3/2}$  and  $S_{1/2}$  using standard relations, including the explicit dependence on  $M_N$  and  $M_R$  [26, 28]. The results are presented in Fig. 2 for the helicity amplitudes and in Fig. 3 for the transition form factors, in comparison with the CLAS data [44, 47, 48] and the Particle Data Group (PDG) data [49].

In the recent years there have been a discussion about the difference between the analysis of JLab and MAID, for the helicity amplitudes associated with the  $N(1520)$  resonance. A detailed discussion can be found in Ref. [26]. From the presentations of V. Burkert, V. Mokeev and L. Tiator [50, 51, 52], we can conclude that this topic is still under discussion.

In Figs. 2 and 3 one can see that the semirelativistic approximation describe very well the empirical data for  $Q^2 > 1.5 \text{ GeV}^2$ , with two exceptions: the amplitude  $A_{3/2}$  and the form factor  $G_E$  for small  $Q^2$ . Apart these cases one can notice that the deviation below  $1.5 \text{ GeV}^2$  is not very significant, suggesting



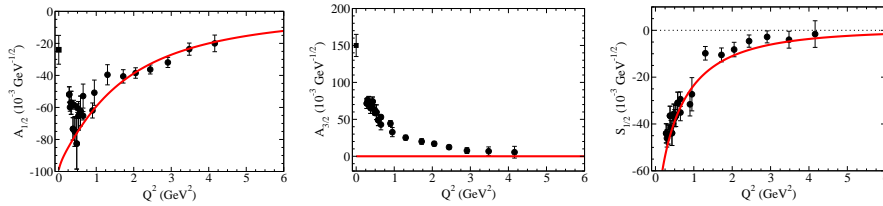


**Fig. 2**  $\gamma^* N \rightarrow N(1520)$  amplitudes. Data from CLAS [44,47,48] and PDG [49].

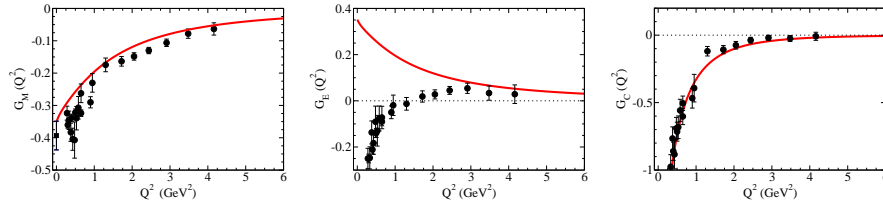


**Fig. 3**  $\gamma^* N \rightarrow N(1520)$  multipole form factors. Data from CLAS [44,47,48] and PDG [49].

small meson cloud effects for the functions  $A_{1/2}$ ,  $S_{1/2}$ ,  $G_M$  and  $G_C$ . For that result contributes the relation  $G_i \propto \frac{T_R}{|\mathbf{q}|}$ , which imply that  $G_M$  and  $A_{1/2}$  are finite in the limit  $Q^2 = 0$  [24].

The failure of the model for  $A_{3/2}$ , where the model predicts  $A_{3/2} \equiv 0$  in contradiction with the significant magnitude of the data, can be interpreted as a limitation of the model calculation, based exclusively on valence quark degrees of freedom [26,28]. The magnitude of the  $A_{3/2}$  data can be an indication that the amplitude is dominated by meson cloud effects. This interpretation is corroborated by calculations from other authors, which conclude that the valence quark contributions can explain only about one third of the observed data. For a more detailed discussion, check Refs. [10,24,26,28] and references therein.

Concerning to the results for  $G_E$ , the failure of the approximation is related to the result  $A_{3/2} = 0$ , and the relation  $A_{3/2} \propto (G_M + G_E)$ , which implies that  $G_M = -G_E$  [26,28].

The interpretation of the results for  $A_{3/2}$  as mainly a consequence of the meson cloud effects, and the conclusion that those effects are not so significant for the other functions, in particular  $A_{1/2}$ , can be used to estimate the magnitude of the meson cloud contributions. The assumption that  $|A_{3/2}^{\text{mc}}| \gg |A_{1/2}^{\text{mc}}|$ , where “mc” label the meson cloud contribution to the amplitudes, implies that [24]:

$$G_E^{\text{mc}} \simeq -\frac{F}{\sqrt{3}} A_{3/2}^{\text{mc}}, \quad G_M^{\text{mc}} \simeq \frac{1}{3} G_E^{\text{mc}}, \quad (12)$$

where  $F = \frac{2M_N}{\sqrt{2\pi\alpha_0}} \sqrt{\frac{M_N(M_R+M_N)}{(M_R-M_N)Q_+^2}}$  and  $Q_+^2 = (M_R + M_N)^2 + Q^2$  ( $\alpha_0$  is the fine structure constant). The previous relations allows then the estimation of the

meson cloud contribution to  $G_E$  in terms of the empirical value of  $A_{3/2}$ , and the conclusion that the effect is much smaller (one third) in the case of  $G_M$ .

In Refs. [26,28] the assumption that  $A_{3/2}$  is dominated by meson cloud effects was used to derive empirical parametrizations for that amplitude. Those parametrizations can then be used in other studies of the  $N(1520)$  systems. An example is the model described in Ref. [28] for the electromagnetic structure of  $N(1520)$  in the timelike region. Another example of the use of those parametrizations is discussed in Sect. 6, in the context of the single quark transition model.

### 3.4 Summary of the results from the semirelativistic approximation

The main conclusion of the results from the semirelativistic approximation is that one can obtain a very good description of the  $Q^2 > 1.5 \text{ GeV}^2$  data taking into account the valence quark contributions. This conclusion is true except for two cases [ $F_2^*$  for  $N(1535)$  and  $A_{3/2}$  for  $N(1520)$ ].

The previous conclusion is impressive, because as mentioned, the input in the semirelativistic approximation is just the parametrization of the nucleon radial wave function and the quark electromagnetic form factors (included on the coefficients  $j_i^S$  and  $j_i^A$ ). To summarize, using exclusively the parametrization of the nucleon structure, one can estimate, with a reasonable precision, the transition form factors for the resonances  $N(1535)$  and  $N(1520)$ .

At small  $Q^2$ , one can still observe a good description of the data, obtaining non-zero results for  $G_E$  and  $G_M$  at the photon point. This result is an indication that the meson cloud effects are in general small, apart the cases mentioned above.

### 3.5 $N(1535)1/2^-$ : relation between $A_{1/2}$ and $S_{1/2}$

The consequence of the result  $F_2^* = 0$ , for  $Q^2 > 1.5 \text{ GeV}^2$  is that, the amplitudes  $A_{1/2}$  and  $S_{1/2}$  are related by [53]

$$S_{1/2} = -\frac{\sqrt{1+\tau}}{\sqrt{2}} \frac{M_R^2 - M_N^2}{2M_R Q} A_{1/2}. \quad (13)$$

The excellent agreement between the  $S_{1/2}$  data and the r. h. s. was confirmed with great precision in the region  $Q^2 = 1.5\text{--}4.2 \text{ GeV}^2$  for the available data [53]. Only future data from JLab-12 GeV upgrade can confirm the accuracy for larger values of  $Q^2$ .

From the theoretical point of view, the result (13) can be interpreted as a consequence of the cancellation between the valence quark contributions and the meson cloud contributions for  $F_2^*$  at large  $Q^2$  [42,53].

Calculations based on the chiral unitary model [54], which use meson-baryon resonance states as effective degrees of freedom, are also consistent with this interpretation. The estimates from the chiral unitary model for  $F_2^*$ , which

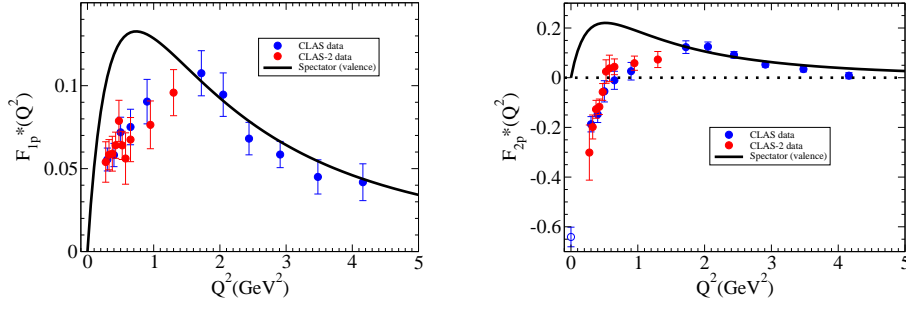


**Fig. 4**  $\gamma^*N \rightarrow N(1440)$  transition form factors for proton target [55,56]. Data from CLAS [44,48] and PDG [49].

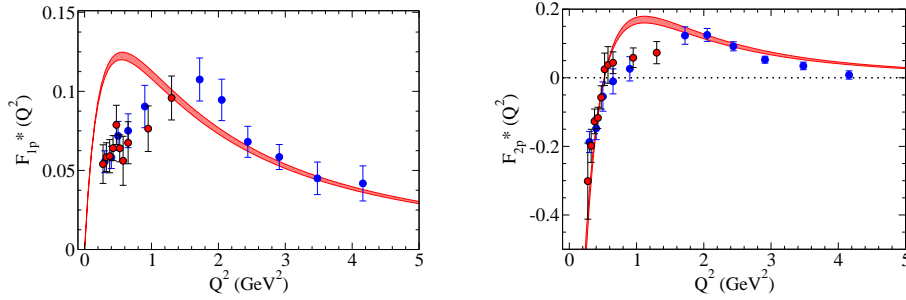


**Fig. 5** Holographic estimate of  $\gamma^*N \rightarrow N(1440)$  transition form factors for proton target [60]. The red bands indicate the interval of values for the form factors, according to the interval of values estimated for the couplings. Data from CLAS [44,48].

can be interpreted as meson cloud contributions, generate results comparable in magnitude with the estimates from the covariant spectator quark model but differ in sign [42,54].

#### 4 $N(1440)1/2^+$

The nucleon first radial excitation, the Roper, can be also described by the covariant spectator quark model. Since  $N(1440)1/2^+$  shares with the nucleon the spin-isospin structure, it differs from the nucleon only by the radial wave function. One can then derive the form of the Roper radial wave function  $\psi_R$  and their relation to the nucleon radial wave function  $\psi_N$  imposing the orthogonality between nucleon and Roper states [55,56]. Because the free parameters are fixed by the orthogonality condition, the expressions obtained for the form factors are true predictions.

The estimates for the form factors are presented in Fig. 4 in comparison with the CLAS data from Refs. [44,48]. The results for the helicity amplitudes are presented later. The estimates for the form factors include only the

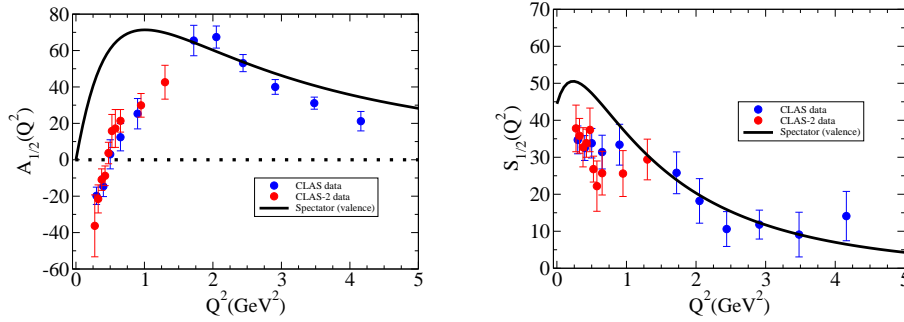


**Fig. 6**  $\gamma^*N \rightarrow N(1440)$  helicity amplitudes for proton target [55,56]. Data from CLAS [44, 48] and PDG [49].

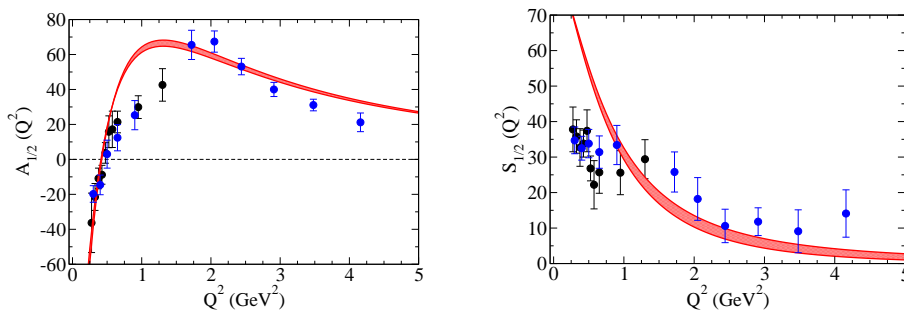


**Fig. 7** Holographic estimate of  $\gamma^*N \rightarrow N(1440)$  helicity amplitudes for proton target [60]. The red bands indicate the interval of values for the form factors, according to the intervals of values estimated for the couplings. Data from CLAS [44,48].

contributions from the valence quarks. In the figure, one can notice that the theoretical results are very close to the empirical data for  $Q^2 > 1.5$  GeV<sup>2</sup>, supporting the assumption that the  $N(1440)1/2^+$  is in fact the first radial excitation of the nucleon [57]. Below 1.5 GeV<sup>2</sup>, the deviation from the data may be interpreted as a manifestation of the meson cloud. In these conditions, one can use our estimate of the quark core contribution to estimate the meson cloud effect from the CLAS data [58].

Recently, the  $\gamma^*N \rightarrow N(1440)$  transition form factors have been estimated using the formalism of Holographic QCD [59]. In this description, the valence quark contributions are interpreted as the contributions from the leading order Fock state associated with a three-valence quark system [60]. The 3 independent couplings are first adjusted by the nucleon elastic form factor data for large  $Q^2$  (small meson cloud effects). The intervals of values obtained for the parameters are used to estimate the  $\gamma^*N \rightarrow N(1440)$  transition form factors, presented in in Fig. 5 (see red band). In the figure we can notice that the holographic estimate describes also very well the large- $Q^2$  region.

The results from Fig. 5 for the Pauli form factor  $F_{2p}^*$  are surprising, because they show an excellent agreement with the low- $Q^2$  data. This result suggests that the meson cloud contributions to  $F_{2p}^*$  may be very small contrarily to what it is usually expected for the transition form factors.

The calibration of the bare couplings determined in Ref. [60] can also be used to derive analytic parametrization to the  $\gamma^*N \rightarrow N(1440)$  transition form factors  $F_{1p}^*$  and  $F_{2p}^*$  [61].

Overall, one can conclude that Holographic QCD is a very promising method to study the  $\gamma^*N \rightarrow N^*$  transitions, since it provides a useful tool to estimate the valence quark effects at small  $Q^2$ .

The results for helicity amplitudes, transverse ( $A_{1/2}$ ) and longitudinal ( $S_{1/2}$ ) corresponding to the transition form factors from Figs. 4 and 5 are presented in the Figs. 6 and 7, for the covariant spectator quark model and the holographic model, respectively. In general, one can observe a good agreement with the data for  $Q^2 > 1.5 \text{ GeV}^2$ , as expected from the analysis of the transition form factors. For the holographic model, in particular, one can observe at small  $Q^2$ , the underestimation of the  $S_{1/2}$  data. This result is mainly the consequence of the model results for  $F_{1p}^*$ , where there is an overestimation of the data at small  $Q^2$  (see Fig. 5). This happens because  $S_{1/2} \propto (F_{1p}^* - \frac{Q^2}{(M_R+M)^2} F_{2p}^*)$ , which implies a reduction of the effect of  $F_{2p}^*$  in this amplitude for small values of  $Q^2$ . A more detailed discussion of the holographic estimates of the helicity amplitudes at small  $Q^2$  can be found in Ref. [61].

## 5 $\Delta(1232)3/2^+$

The  $\gamma^*N \rightarrow \Delta(1232)$  is characterized by the 3 multipole form factors: the magnetic dipole ( $G_M^*$ ), the electric quadrupole ( $G_E^*$ ) and the Coulomb quadrupole ( $G_C^*$ ) [7, 8, 62]. According with the  $SU(6)$  symmetry, the  $\gamma^*N \rightarrow \Delta(1232)$  transition is predominantly a magnetic transition, as a consequence of a spin-flip of a quark on the nucleon to create the  $\Delta(1232)$  (spin 3/2) [34]. As a result,  $G_M^*$  is the dominant form factor in the transition.

There are, however, also contributions from the quadrupole form factors,  $G_E^*$  and  $G_C^*$ . The contributions of these form factors for the transition cross-section are determined by the functions  $G_E^*$  and  $\frac{|\mathbf{q}|}{2M_\Delta} G_C^*$ , and have therefore a small impact ( $|\mathbf{q}|$  is the photon three-momentum and  $M_\Delta$  is the  $\Delta(1232)$  mass) [8, 11, 63, 64, 65, 66].

The small but nonzero contributions for  $G_E^*$  and  $\frac{|\mathbf{q}|}{2M_\Delta} G_C^*$  can be interpreted as an indication of the deformation from the  $\Delta(1232)$  [38, 67, 68, 69]. The present results for the quadrupole form factors are compatible with an oblate shape for the  $\Delta^+(1232)$  [38, 68]. The estimate of the valence quark contributions for the  $\Delta^+(1232)$  spacial density is presented in Fig. 8. In the figure, one can confirm the expected deformation along the horizontal axis for the  $\Delta^+(1232)$  (the vertical axis is defined by the spin projection:  $S_z = +\frac{3}{2}$ ) [38].

In the following, we discuss the results for the  $\gamma^*N \rightarrow \Delta(1232)$  form factors based on the calculations from the covariant spectator quark model.

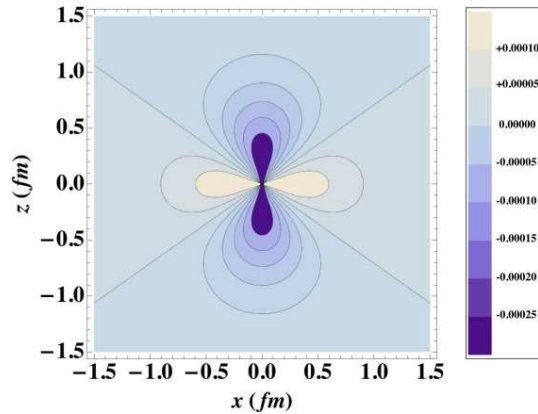


**Fig. 8** Visualization of the  $\Delta^+(1232)$  deformation. The density is defined for the maximum spin projection  $S_z = +\frac{3}{2}$  [38]. The lighter regions correspond to the larger values (the scale is defined on the right side).

### 5.1 Magnetic dipole form factor

The magnetic dipole form factor is in general dominated by the valence quark contributions, consistently with estimates based on  $SU(6)$ , where the quarks are described by  $S$ -states [34, 70]. It is well known, however, that models based on valence quarks underestimate the experimental data in about 40% at low  $Q^2$  [34, 35, 36, 70]. This subject was also discussed in the presentations from H. Kamano and V. Burkert [46, 50].

The missing strength in the form factor  $G_M^*$  is in general interpreted as the consequence of the meson cloud, dominated the lightest meson, the pion, which is not taken into account in quark model calculations [7, 34, 35, 36]. In the case of the covariant spectator quark model, this underestimation can be naturally explained when we consider a simple model where the nucleon and the  $\Delta(1232)$  are described by  $S$ -states for the quark-diquark system. In these conditions the quadrupole form factors have no contributions ( $G_E^* = G_C^* \equiv 0$ ) and only the magnetic dipole form factor have non-zero results [7]. The magnetic dipole form factor can then be calculated using the a simple expression [7, 8]:

$$G_M^*(Q^2) = \frac{4}{3\sqrt{3}} \frac{M_N}{M_\Delta + M_N} \left[ f_{1-} + \frac{M_\Delta + M_N}{2M_N} f_{1-} \right] \int_k \psi_\Delta \psi_N \quad (14)$$

where  $f_{1-}$  and  $f_{2-}$  are the quark Dirac and Pauli isovector form factors and  $\psi_N$ ,  $\psi_\Delta$  are the nucleon and  $\Delta(1232)$  radial wave functions. Based on the previous relation, one can conclude, using the normalization conditions, the Cauchy-Schwartz inequality,  $\int_k \psi_\Delta \psi_N \leq 1$ , and the values of the quark anomalous magnetic moments, that  $G_M^* \leq 2.07$  for  $Q^2 = 0$  [7, 31].

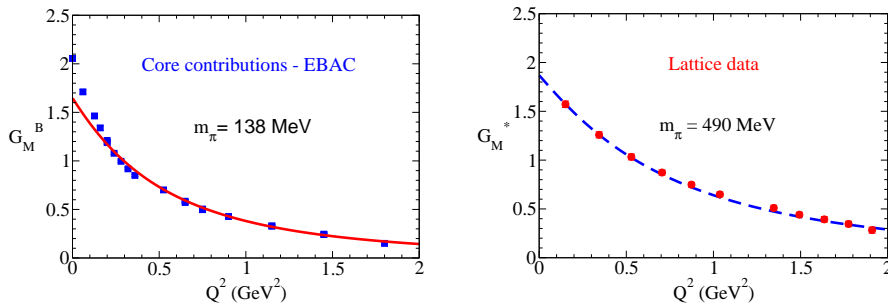


**Fig. 9** **At the right:** Comparison with EBAC estimate of bare core [34]. **At the left:** Extrapolation to the lattice QCD regime with  $m_\pi = 490$  MeV. Lattice data from Ref. [71].

Since the experimental value is  $G_M^*(0) \simeq 3.02$  [49], one can conclude that near  $Q^2 = 0$ , the model underestimates the data in about 37%. Note that this estimate provide only an upper limit, and that in practice, one can have even larger underestimations [7, 31].

From the previous discussion, we can conclude that the covariant spectator quark model provides a natural explanation for the underestimation of the data at low  $Q^2$ , when we consider only the valence quark degrees of freedom. In order to explain the missing strength, one needs to take into account explicit contributions of the pion cloud effects, as concluded from the use of dynamical baryon-meson reaction models [2, 7, 34, 35, 36].

Before explaining how one can parametrize the pion cloud effects, one needs to discuss how we can parametrize the of the nucleon and the  $\Delta(1232)$  wave functions. As discussed in Sect. 2, the structure of the nucleon can be described within the covariant spectator quark model, considering an  $SU(6)$  structure for the  $S$ -state wave function, and a parametrization for the quark current (1) [6]. As for the nucleon, we consider also an  $S$ -state structure associated with a radial wave function  $\psi_\Delta$  [7, 8, 11]. The question is, how to determine the function  $\psi_\Delta$ , since, contrary to the nucleon elastic form factors, the radial wave function cannot be adjusted directly to the empirical data, because the data is strongly contaminated by pion cloud effects.

We are then left with two options: i) calibrate the data by some estimate from the valence quark core contributions to the transition form factors; ii) calibrate the model by lattice QCD simulations for large pion masses, where the meson cloud effects are suppressed.

The first option can be implemented using the estimate of the quark core contributions performed with the assistance of the Sato-Lee/EBAC model, nowadays known as Argonne-Osaka model [33, 34, 37, 46]. The second option requires an intermediate step, the extension of the covariant spectator quark model from the physical regime to the lattice QCD regime. This extension can be performed taking advantage of the definition of the quark currents in terms of the hadron masses (vector mesons and nucleon mass) and also

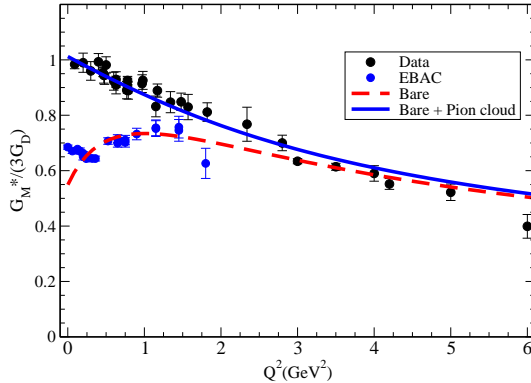


**Fig. 10** Combination of valence (Bare) and pion cloud contributions for  $G_M^*$  [11]. The valence quark contributions are the same as in Fig. 9. The pion cloud contribution is estimated by Eq. (15). The blue bullets represent the EBAC estimate of the quark core [34], as before.

the convenient definition of the radial wave functions in terms of the mass of the baryons under study. The discussion about the extension of the covariant spectator quark model for lattice QCD can be found in Refs. [9, 11, 18, 22, 27].

The results from the covariant spectator quark model for  $G_M^*$  are presented in Fig. 9. The parameters of the model are adjusted to the EBAC estimate of the bare core in Ref. [8]. The results are presented in the left panel, where  $G_M^*$  is relabeled as  $G_M^B$  ( $B$  holds for bare), since no pion cloud contributions are taken into account. The label  $m_\pi = 138$  MeV is included to remind that the calculation is performed at the physical point. The model was later extended to the lattice QCD regime using the same parametrization for  $\psi_\Delta$  [11]. The extension of the model gives as accurate description of the lattice QCD data for  $m_\pi = 411, 490$  and  $563$  MeV [71]. The results for  $m_\pi = 490$  MeV are presented in the left panel of Fig. 9.

Since the parametrization for  $\psi_\Delta$  gives a simultaneously good description of the EBAC estimate of the bare core contribution, and of the lattice data for  $m_\pi > 0.4$  GeV, a region where we expect very small pion cloud effects, we can conclude that we have a consistent description of the physics associated with the valence quark degrees of freedom.

How to simulate the pion cloud ?

As discussed above, if we want to describe the  $\gamma^* N \rightarrow \Delta(1232)$  magnetic dipole form factor in all range of  $Q^2$ , one needs to take into account the mechanism of the pion cloud.



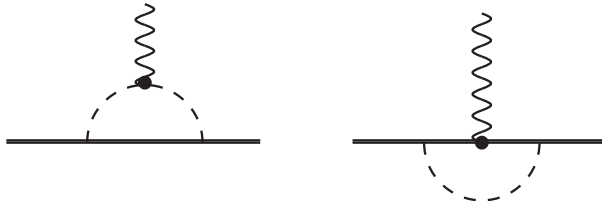


**Fig. 11** Diagrammatic representation of first contributions to the pion cloud contributions. The first diagram represents the photon coupling with the pion (includes function  $F_\pi$ ). The second diagram simulates the photon interaction with intermediate baryon states.

In our first attempt, we considered a simple phenomenological parametrization of the pion cloud contribution to  $G_M^*$ ,  $G_M^\pi$ , in the form [7, 8, 11]

$$\frac{G_M^\pi}{3G_D} = \lambda_\pi \left( \frac{\Lambda_\pi^2}{\Lambda_\pi^2 + Q^2} \right)^2, \quad (15)$$

where  $G_D = 1/(1 + Q^2/0.71)^2$  is the dipole form factor,  $\lambda_\pi$  define the strength of the contribution, and  $\Lambda_\pi^2$  is a cutoff that define the falloff. The best description of the data is obtained for  $\lambda_\pi = 0.441$  and  $\Lambda_\pi^2 = 1.53 \text{ GeV}^2$  [8].

The representation (15) is motivated by the usual representation of  $G_M^*$ , normalized by the factor  $3G_D$ , and also for the expected falloff from perturbative QCD (pQCD). Based on pQCD arguments one can conclude that a contribution associated with the pion on a three-quark system, and represented by a  $q\bar{q}$  state is described by a function  $\propto 1/Q^{2(3+2-1)} = 1/Q^8$ , where the extra 2 is the consequence of the additional  $q\bar{q}$  state [72].

The result of the parametrization  $G_M^\pi$ , combined with the valence quark contributions discussed in the previous section (see Fig. 9) is presented in Fig. 10, up to  $6 \text{ GeV}^2$ . In the figure, one can see that the bare contributions give a good description of the data when  $Q^2 > 3 \text{ GeV}^2$  (small pion cloud).

Once tested the parametrization to the pion cloud component, one can use it in calculations associated with the  $\gamma^*N \rightarrow \Delta(1232)$  transition. The parametrization was used, in particular in the calculation of the octet to decuplet transition form factors [31, 32], and also in the calculation of the  $\gamma^*N \rightarrow \Delta(1600)$  transition form factors [43]. An extension of Eq. (15) with minor modifications was used in the calculation of the  $\gamma^*N \rightarrow \Delta(1232)$  transition in the timelike regime [29].

In the more recent studies of the  $\gamma^*N \rightarrow \Delta(1232)$  transition, we considered an improved form of the parametrization (15). One considers in particular the form [30]

$$G_M^\pi(q^2) = 3 \frac{\lambda_\pi}{2} F_\pi(q^2) \left( \frac{\Lambda_\pi^2}{\Lambda_\pi^2 - q^2} \right)^2 + 3 \frac{\lambda_\pi}{2} \left[ \frac{\Lambda_D^4}{(\Lambda_D^2 - q^2)^2 + \Lambda_D^2 \Gamma_D^2(q^2)} \right]^2, \quad (16)$$

where  $F_\pi(q^2)$  is the empirical pion electromagnetic form factor,  $\Lambda_D^2 = 0.9 \text{ GeV}^2$  is the nucleon dipole cutoff, and  $\Gamma_D$  is a phenomenological width. In this case

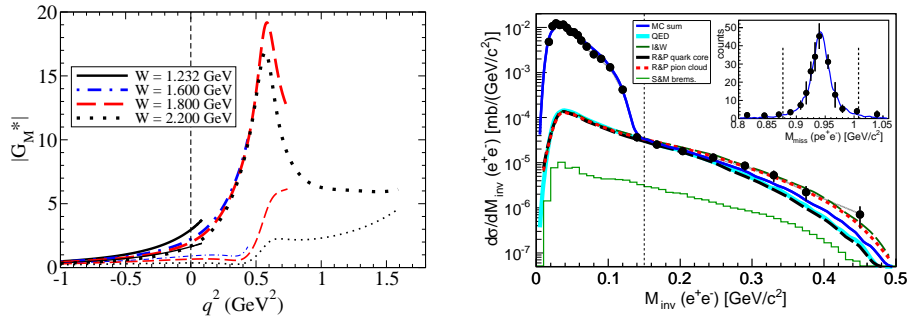


**Fig. 12** At the right: Calculation of  $|G_M^*|$  in timelike region in terms of  $W$  [30]. At the left:  $\Delta(1232)$  Dalitz decay cross-sections from HADES [77]. See discussion in the main text.

the functions are represented in terms of  $q^2 = -Q^2$ , in order to facilitate the discussion in the timelike regime. The new parametrization improves the previous one, because it clearly separates the contributions from the photon coupling with the pion from the photon coupling with intermediate baryon states (see Fig. 11).

The motivation for the use of the parametrization (16) is based on the diagrammatic representation of Fig. 11, and in the results of the study of the octet to decuplet transition from Ref. [32]. In that work a microscopic meson cloud contribution based on the cloudy bag model [73] was used in combination with the covariant spectator quark model for the quark core. It was found that in the case of the  $\gamma^*N \rightarrow \Delta(1232)$  transition each diagram contribute with about 50% to the pion cloud effect.

In the new representation only a part (50%) of the contribution is then linked with the photon coupling with the pion, as expected in a realistic description. The second term, which describes the coupling with intermediate baryons is now represented phenomenologically, using an effective generalization of  $G_D^2$  to the timelike region, where the pole  $q^2 = \Lambda_D^2$  is regularized [29, 30].

The present representation of  $G_M^\pi$  is particularly useful for studies in the timelike region, in particular to the study of the  $\Delta(1232)$  Dalitz decay:  $\Delta \rightarrow \gamma^*N \rightarrow e^+e^-N$ , where the final state has a dilepton pair [30, 74]. These processes have been studied at HADES [74, 75, 76, 77]. This topic was discussed also in the presentation of B. Ramstein [78].

In the timelike region, one can calculate the  $G_M^*$  form factor, which is complex, in terms of the running mass  $W$  that can differ from the mass of the pole  $M_\Delta$ . The results of  $|G_M^*|$  for different values of  $W$  are presented in the left panel of Fig. 12. For kinematic reasons the functions are limited by  $q^2 \leq (W - M)^2$  [29, 30]. The model for  $|G_M^*|$  was used to estimate the  $\Delta(1232)$  Dalitz cross-sections and it was compared with the results from HADES [77]. The results are presented in the right panel of Fig. 12. The covariant spectator

quark model (dashed black line) gives a very good description of the data below  $0.15 \text{ GeV}/c^2$  but underestimates the data for large values of the  $e^+e^-$  invariant mass. The description of the higher region is achieved when we take into account only the pion cloud contributions (dotted red line) [77].

It is expected that in a near future the experimental study of the Dalitz decays can be extended to the  $N(1520)$  [28].

## 5.2 Quadrupole form factors

Also for the quadrupole form factors we can consider a decomposition between the bare and pion cloud contributions. The main difference is that in this case the bare contributions are very small, because those contributions are the consequence of small  $D$ -state mixtures in the  $\Delta(1232)$  wave function. There are two  $D$ -state to be considered in the  $\Delta(1232)$ : one where the sum of the quark spin (core spin) is  $1/2$ ; another where the core spin is  $3/2$ . The  $D$ -state associated with the core spin  $3/2$  gives the dominant contribution to  $G_E^*$ . The  $D$ -state associated with the core spin  $1/2$  gives the dominant contribution to  $G_C^*$  [8]. An accurate description of the lattice QCD data favors a mixture of  $0.72\%$  for both  $D$ -states [11]. The corresponding results for the form factors at the physical limit ( $m_\pi = 138 \text{ MeV}$ ) are presented in Fig. 13 by the dashed-line. In the same figure we present also the lattice QCD data from Ref. [71] for  $m_\pi = 411, 490$  and  $591 \text{ MeV}$ . From the figure it is clear that the estimate of the valence quark contributions and the lattice QCD data is way below the physical data, represented by the dark bullets. Near  $Q^2 = 0$  the valence quark contributions explain only about  $10\text{--}20\%$  of the measured data [11,63].

The predictions approach the experimental data only when we include the contributions of the pion cloud. In the literature, there are simple parametrizations of the pion cloud contributions to the form factors  $G_E^*$  and  $G_C^*$ , derived in the large  $N_c$  limit [79,80]. These relations estimate the pion cloud contributions for the quadrupole form factors based on parametrizations of the neutron electric form factor  $G_{En}$ . The result of the combination of valence quark and pion cloud contributions is presented in Fig. 13 by the solid line. From the final result, we can conclude that the pion cloud effects dominate both form factors.

It is important to note that the estimates of pion cloud contributions, are valid only for small  $Q^2$ , because they are derived from the low  $Q^2$  expansion  $G_{En} \simeq -\frac{1}{6}r_n^2 Q^2$ , where  $r_n^2$  is the neutron electric square radius [79]. It is expected that those contributions are suppressed for very large  $Q^2$  comparative to the valence quark contributions, according with the pQCD falloffs  $G_E^* \propto 1/Q^4$  and  $G_C^* \propto 1/Q^6$  [63,64,72].

From the figure, we can also conclude that there is an excellent agreement between model and data when we combine the two effects. This agreement is impressive because there is no direct fit to the data. The valence quark contribution is estimated exclusively by the lattice QCD data, and the pion cloud contribution is estimated by parameter free expressions [79].

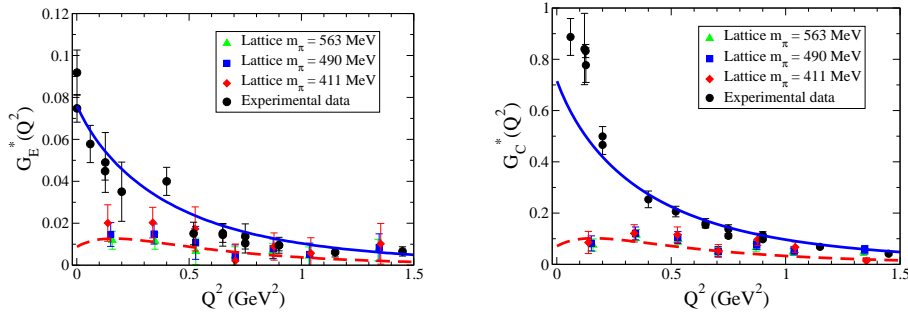


**Fig. 13** At the right: Results for  $G_E^*$ . At the left: Results for  $G_C^*$ . In both cases the dashed-line represent the bare contribution (at the physical point) and the solid-line the combination of the bare and pion cloud. Lattice QCD data from Ref. [71]. The description of the data can be found in Ref. [11].

Only at low  $Q^2$  one can observe some deviation for  $G_C^*$  below  $0.15 \text{ GeV}^2$ . This gap between theory and empirical data has been discussed in the literature [63,64,65]. It was recently shown that the  $G_C^*$  data have been overestimated. The new measurements and the recent data analysis evidence a reduction in the values for  $G_C^*$  below  $0.15 \text{ GeV}^2$  [81]. The result of a new analysis of JLab/Hall A was presented during the workshop by N. Sparveris [82].

### 5.3 Siegert's theorem

An interesting discussion about the  $\gamma^* N \rightarrow \Delta(1232)$  quadrupole form factors is raised when we consider Siegert's theorem [4,83,84,85]. Siegert's theorem states that the electric and the Coulomb quadrupole form factors are related at the pseudthreshold when the nucleon and the  $\Delta(1232)$  are both at rest, by [62,66,86]

$$G_E^*(Q_{pt}^2) = \frac{M_\Delta - M_N}{2M_\Delta} G_C^*(Q_{pt}^2), \quad (17)$$

where  $Q_{pt}^2 = -(M_\Delta - M_N)^2$ . In the following discussion, we use  $\kappa = \frac{M_\Delta - M_N}{2M_\Delta}$ .

When expressed in terms of the scalar ( $S_{1/2}$ ) and the electric ( $E_{1+}$ ) amplitudes, Eq. (17) implies  $E_{1+} = \sqrt{2}(M_\Delta - M_N)S_{1/2}/|\mathbf{q}|$  [66,86]. The previous relation is violated by previous MAID parametrizations [4,84]. In Ref. [86] it is discussed in detail how the helicity amplitudes can be parametrized in order to satisfy the condition (17). The discussion of Siegert's theorem can also be extended to the  $N(1535)$  and  $N(1520)$  systems [66,86].

It was recently shown that the parametrizations proposed to estimate the pion cloud effects [79] are not fully compatible with Siegert's theorem in the form of Eq. (17) [63]. For the purpose of the discussion, it is convenient to

write the pion cloud contributions for the quadrupole form factors in the form

$$G_E^\pi = \left(\frac{M}{M_\Delta}\right)^{3/2} \frac{M_\Delta^2 - M_N^2}{2\sqrt{2}} \frac{\tilde{G}_{En}}{1 + \alpha}, \quad G_C^\pi = \left(\frac{M_N}{M_\Delta}\right)^{1/2} \sqrt{2} M_\Delta M_N \tilde{G}_{En}, \quad (18)$$

where  $\tilde{G}_{En} = G_{En}/Q^2$ , and  $\alpha$  is a function to be discussed next. The original form proposed by Pascalutsa and Vanderhaeghen has  $\alpha \equiv 0$  [79].

To measure the error in Eq. (17), we use  $\mathcal{R}_{pt} \equiv G_E^*(Q_{pt}^2) - \kappa G_C^*(Q_{pt}^2)$ . An exact description of Eq. (17) implies that  $\mathcal{R}_{pt} = 0$ .

Starting with the original parametrizations (18), where  $\alpha = 0$ , one can conclude using the approximation  $G_{En} \simeq -\frac{1}{6}r_n^2 Q^2$  for small values of  $Q^2$  (including  $Q_{pt}^2$ ), that  $\mathcal{R}_{pt} = \mathcal{O}(1/N_c^2)$ . An error  $\mathcal{R}_{pt} = \mathcal{O}(1/N_c^2)$  can be significant in numerical calculations [63].

It was found that the description of Siegert's theorem and the data can be improved when we consider  $\alpha = \frac{Q^2}{M_\Delta^2 - M_N^2}$  [63]. In that case we can write  $\mathcal{R}_{pt} = \left(\frac{M_\Delta}{M_N}\right)^{\frac{3}{2}} \frac{M_\Delta - M_N}{2M_N} \frac{r_n^2}{12\sqrt{2}} Q_{pt}^2$  corresponding to a term  $\mathcal{O}(1/N_c^4)$  [63], a negligible violation of Siegert's theorem. The results for  $G_E^*$  and  $\kappa G_C^*$  are presented in the left panel of Fig. 14. The almost convergence of  $G_E^*$  and  $\kappa G_C^*$  for the lowest value of  $Q^2$  is an indication of the almost validity of Siegert's theorem.

To the agreement with the data contribute also the inclusion of the valence quark component, as discussed previously relative to the results from Fig. 13. The advantage of the estimate of valence quark contribution with a covariant quark model is that the contributions for the quadrupole form factors  $G_E^*$  and  $G_C^*$  vanishes at the pseudothreshold, as a consequence of the orthogonality between nucleon and  $\Delta(1232)$  states [8, 11, 63].

The previous result,  $\mathcal{R}_{pt} = \mathcal{O}(1/N_c^4)$ , was improved in a more recent work [64]. We obtain an exact description of Siegert's theorem when we consider  $\alpha = \frac{Q^2}{2M_\Delta(M_\Delta - M)}$ , which correspond to a correction of the previous representation by a term  $\mathcal{O}(1/N_c^4)$  at the pseudothreshold. When combined with the valence quark contribution, one obtains again a good agreement with the quadrupole form factor data. The results for  $G_E^*$  and  $\kappa G_C^*$  are present in the right panel of Fig. 14, in comparison with the data from Refs. [81, 87].

The agreement from the right panel of Fig. 14 is more impressive because we include the most recent data for  $G_C^*$  from JLab/Hall A, below 0.15 GeV<sup>2</sup> (see full circles and full diamonds). When we consider the new data we obtain, at last, a consistent description of the quadrupole form factor data at low  $Q^2$ .

We recall that for this agreement contributes the inclusion of a valence quark component estimated by a covariant quark model calibrated by lattice QCD data (no pion cloud contamination) [11] and an improved parametrizations of the pion cloud contributions to the quadrupole form factors with no adjustable parameters.

More recently, the relations (18) with  $\alpha = \frac{Q^2}{2M_\Delta(M_\Delta - M_N)}$  have used to study alternative parametrizations for the neutron electric form factor  $G_{En}$  [65].

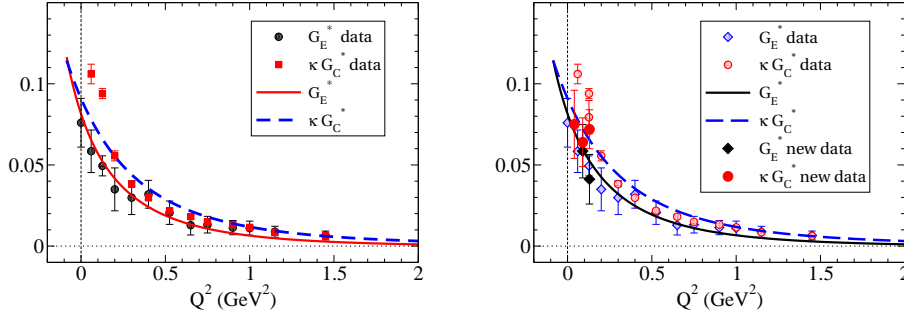


**Fig. 14** Siegert's theorem. **At the right:** Results from Ref. [63]. **At the left:** Results from Ref. [64]. Data from Ref. [87]. The new data are from JLab/Hall A (solid circles and solid diamonds) [81].

#### 5.4 Summary of the $\Delta(1232)3/2^+$ results

We can now summarize the covariant spectator quark model results for the  $\gamma^*N \rightarrow \Delta(1232)$  transition.

We conclude that the simplest model, where the nucleon and the  $\Delta(1232)$  are described by quark-diquark  $S$ -states, is consistent with the results for  $G_M^*$  from lattice QCD simulations and with estimates from the bare core effects based on the EBAC/Argonne-Osaka dynamical model.

When we take into account  $D$ -states in the  $\Delta(1232)$  one obtain also a consistent description of  $G_M^*$  and the quadrupole form factors  $G_E^*$  and  $G_C^*$ .  $G_M^*$  is dominated by valence quark contributions. The quadrupole form factors are dominated by pion cloud contributions.

The present model for  $G_M^*$ , including the parametrization of the pion cloud contribution ( $G_M^{\pi}$ ) can be used as input in calculations of other processes. Examples of that are the extension of the model to the timelike region ( $\Delta(1232)$  Dalitz decay) [29,30], and the octet to decuplet transitions [31,32]. The model for the  $\Delta(1232)$  structure can also be used to calculate  $\Delta(1232)$  elastic form factors [9,38,39,40].

## 6 Results for the $[70, 1^-]$ supermultiplet

One can estimate the helicity amplitudes of the resonances from the  $[70, 1^-]$  supermultiplet with the help of the single transition quark model (SQTM) [10, 88, 89, 90]. According to the  $SU(6) \otimes O(3)$  classification the components of the  $[70, 1^-]$  supermultiplet are particles and angular momentum  $J = \frac{1}{2}, \frac{3}{2}$  and negative parity. More explicitly, the supermultiplet includes the resonances  $N(1535)1/2^-$  and  $N(1520)3/2^-$  discussed previously in Sect. 3, in addition to  $N(1650)1/2^-$ ,  $N(1700)3/2^-$ ,  $\Delta(1620)1/2^-$  and  $\Delta(1700)3/2^-$ .

The SQTM assumes that in the electromagnetic interaction the photon couples with a single quark, and that the wave functions of the baryons are

described by the  $SU(6) \otimes O(3)$  symmetry group. In these conditions one can express the quark transverse current in the form [90]

$$J^+ = AL^+ + B\sigma^+L_z + C\sigma_zL^+ + \dots, \quad (19)$$

where  $L$  is the orbital angular operator,  $\sigma$  is the Pauli spin operator, and  $A$ ,  $B$  and  $C$  are functions of  $Q^2$ . The operator act on the quark spatial wave functions. The dots represent an extra term relevant for other supermultiplets but that is absent for the  $[70, 1^-]$  supermultiplet.

As a consequence from Eq. (19) the transverse helicity amplitudes of the transition  $\gamma^*N \rightarrow N^*$ , where  $N^*$  is a member of the  $[70, 1^-]$  supermultiplet, can be represented in terms of the three independent functions  $A$ ,  $B$  and  $C$ , and two mixture angles  $\theta_S$  and  $\theta_D$  determined experimentally [10,16,90]. The relation between the amplitudes and the coefficients can be found in Ref. [10].

The coefficients  $A$ ,  $B$  and  $C$  can be determined for the case of proton targets using the available data for finite  $Q^2$  associated with three amplitudes for some resonances  $N^*$  from the supermultiplet. We choose then the amplitudes associated with the states  $N(1535)1/2^-$  ( $A_{1/2}^S$ ) and  $N(1520)3/2^-$  ( $A_{1/2}^D$  and  $A_{3/2}^D$ ) calculated within the covariant spectator quark model from Refs. [25, 26,28]. One can combine the frameworks from the SQTM with the covariant spectator quark model because both frameworks are based on the  $SU(6)$  wave functions and on the impulse approximation. However, since both frameworks are restricted to the valence quark degrees of freedom we cannot expect the estimates to hold for small  $Q^2$ .

In Refs [10,25,26,28] the valence quark contributions to the transition form factors and helicity amplitudes for  $N(1535)1/2^-$  and  $N(1520)3/2^-$  are calculated in terms of the radial wave functions of the resonance. Adjusting just one parameter of the radial wave functions per resonance, associated with the long range behavior, one can reproduce the helicity amplitude data for  $Q^2 > 2 \text{ GeV}^2$ , with a minor exception. The amplitude  $A_{3/2}$  for the state  $N(1520)3/2^-$  cannot be described in the context of the covariant spectator quark model, which predicts  $A_{3/2}^D = 0$ , as mentioned in Sect. 3. As discussed, the result  $A_{3/2}^D = 0$  can be interpreted as a manifestation that the amplitude  $A_{3/2}^D$  is dominated by meson cloud effects [10,26,28].

The interpretation of  $A_{3/2}^D$  as the representation of the meson cloud contributions can be used to identify the meson cloud contributions to the remaining amplitudes of the supermultiplet, tracking the contribution of  $A_{3/2}^D$  on those amplitudes. By subtraction one can also identify the valence quark contributions [10].

In Fig. 15, we present the results for the amplitudes associated with the states  $N(1650)1/2^-$  and  $\Delta(1620)1/2^-$ , in comparison with the data from CLAS, MAID and PDG. Predictions for the resonances  $N(1700)3/2^-$  and  $\Delta(1700)3/2^-$  are presented in Ref. [10]. We do not discuss those results here because the data for  $Q^2 > 1 \text{ GeV}^2$  are scarce or nonexistent [10]. In Fig. 15, one can observe a good general agreement between the estimate based on the SQTM and the data. There is, however, an important difference between the

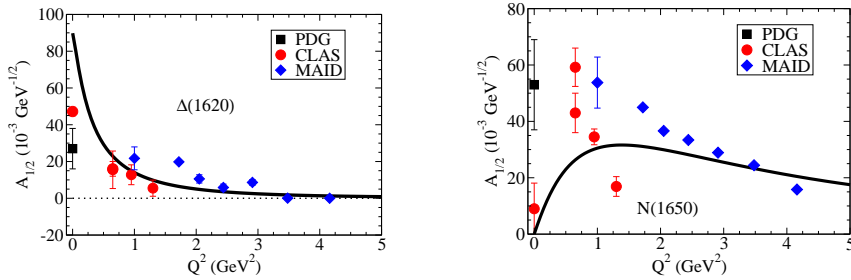


**Fig. 15** Results from the parametrization from SQTm. **At left:**  $\Delta(1620)1/2^-$ . **At right:**  $N(1650)1/2^-$ . Data from Refs. [4, 44, 47, 49, 91, 92].

two results. The  $N(1650)1/2^-$  amplitude is independent of the parametrization  $A_{3/2}^D$ , meaning that the result is the same when we drop the contribution of that amplitude ( $A_{3/2}^D \rightarrow 0$ ). As for the  $\Delta(1620)1/2^-$  amplitude, the contributions associated with the amplitudes  $A_{1/2}^S$  and  $A_{1/2}^D$  cancel almost exactly. One concludes, then that  $A_{1/2} \propto A_{3/2}^D$ , meaning that the SQTm cannot predict  $A_{1/2}$  for  $\Delta(1620)1/2^-$ , unless the meson cloud effects are included explicitly. For a more detailed, discussion check Ref. [10]. Since the data available for the  $\Delta(1620)1/2^-$  for large  $Q^2$  are restricted to the MAID data, which have abnormally small errorbars, it will be very interesting to see if the future data from the JLab-12 GeV upgrade confirms or deny the present trend of the calculations. The same observation holds for  $N(1650)1/2^-$  amplitude and for the amplitudes associated with the resonances  $N(1700)3/2^-$  and  $\Delta(1700)3/2^-$ , discussed in Ref.[10].

The results of SQTm framework based on the covariant spectator quark model results from Refs. [25, 26, 28] with adjustable radial wave function  $\psi_R$  can in a near future be improved based on the covariant spectator quark model results in the semirelativistic limit (Sect. 3). In that case, we can obtain parametrizations to the  $[70, 1^-]$  supermultiplet which depend only on the nucleon parametrization for the radial wave function  $\psi_N$ .

## 7 Summary and conclusions

We present here covariant estimates for the transition form factors and the helicity amplitudes for several nucleon excitations  $N^*$ . We discussed, in particular the results for the resonances  $\Delta(1232)3/2^+$ ,  $N(1440)1/2^+$ ,  $N(1535)1/2^-$  and  $N(1520)3/2^-$  as well as results for the resonances of  $[70, 1^-]$  supermultiplet,  $\Delta(1620)1/2^-$  and  $N(1650)1/2^-$ , based on a connection with the single quark transition model.

In general, we observed a good agreement between model predictions and empirical data at large  $Q^2$ . This result can be interpreted as an indication



that the effects of the valence quark degrees of freedom in the model are under control.

For the  $\Delta(1232)3/2^+$  there is today a convergence of results from different methods, including lattice QCD simulations, quark models, Dyson-Schwinger equations and also from dynamical coupled-channel models.

As for the other resonances, the estimates based on different methods are still under debate. At the moment, the best that we can do, for sure, is to make predictions for large  $Q^2$ .

Based on the results obtained within the framework of the covariant spectator quark model, we can conclude that the meson cloud effects may be relevant at moderated  $Q^2$  (region around  $Q^2 \approx 2 \text{ GeV}^2$ ) for some resonances  $N^*$ . Here we discussed the Pauli form factor for the resonance  $N(1535)1/2^-$ , and the amplitude  $A_{3/2}$  for the resonance  $N(1520)3/2^-$ .

In the near future we can expect developments related to the following topics:

- New data at large  $Q^2$  and more precise data at any range can help the interpretation of the empirical results. In this context the coming results from the JLab-12 GeV-upgrade may be particularly relevant.
- Lattice QCD simulations below the  $N^*$  threshold will help to refine the interpretation of our theoretical models based on valence quark and meson cloud degrees of freedom.
- New estimates of the bare core contributions to the transition form factors based on dynamical couple-channel models and the comparison with estimates from quark models can help to understand the data for several resonances  $N^*$ . This comparison was already very useful in the past for the  $\Delta(1232)3/2^+$ , as discussed in the present work.

**Acknowledgements** The author thanks Adolf Buchmann, Ralf Gothe, Viktor Mokeev, Beatrice Ramstein, Elena Santopinto and Nikolaos Sparveris for helpful discussions and Witold Przygoda and the HADES collaboration the results from Ref. [77] (right panel of Fig. 12). This work was supported by the Fundação de Amparo à Pesquisa do Estado de São Paulo (FAPESP): project no. 2017/02684-5, grant no. 2017/17020-BCO-JP.

## References

1. I. G. Aznauryan, A. Bashir, V. Braun, S. J. Brodsky, V. D. Burkert, L. Chang, C. Chen and B. El-Bennich *et al.*, Studies of Nucleon Resonance Structure in Exclusive Meson Electroproduction, *Int. J. Mod. Phys. E* **22**, 1330015 (2013)
2. V. D. Burkert and T. S. H. Lee, Electromagnetic meson production in the nucleon resonance region, *Int. J. Mod. Phys. E* **13**, 1035 (2004)
3. I. G. Aznauryan and V. D. Burkert, Electroexcitation of nucleon resonances, *Prog. Part. Nucl. Phys.* **67**, 1 (2012)
4. D. Drechsel, S. S. Kamalov and L. Tiator, Unitary Isobar Model – MAID2007, *Eur. Phys. J. A* **34**, 69 (2007); L. Tiator, D. Drechsel, S. S. Kamalov and M. Vanderhaeghen, Baryon Resonance Analysis from MAID, *Chin. Phys. C* **33**, 1069 (2009)
5. G. Eichmann, H. Sanchis-Alepuz, R. Williams, R. Alkofer and C. S. Fischer, Baryons as relativistic three-quark bound states, *Prog. Part. Nucl. Phys.* **91**, 1 (2016)
6. F. Gross, G. Ramalho and M. T. Peña, A Pure  $S$ -wave covariant model for the nucleon, *Phys. Rev. C* **77**, 015202 (2008)

7. G. Ramalho, M. T. Peña and F. Gross, A Covariant model for the nucleon and the  $\Delta$ , Eur. Phys. J. A **36**, 329 (2008)
8. G. Ramalho, M. T. Peña and F. Gross,  $D$ -state effects in the electromagnetic  $N\Delta$  transition," Phys. Rev. D **78**, 114017 (2008)
9. G. Ramalho, K. Tsushima and F. Gross, A Relativistic quark model for the  $\Omega^-$  electromagnetic form factors, Phys. Rev. D **80**, 033004 (2009)
10. G. Ramalho, Using the Single Quark Transition Model to predict nucleon resonance amplitudes, Phys. Rev. D **90**, 033010 (2014)
11. G. Ramalho and M. T. Peña, Valence quark contribution for the  $\gamma N \rightarrow \Delta$  quadrupole transition extracted from lattice QCD, Phys. Rev. D **80**, 013008 (2009)
12. F. Gross, Three-dimensional covariant integral equations for low-energy systems, Phys. Rev. **186**, 1448 (1969); F. Gross, J. W. Van Orden and K. Holinde, Relativistic one boson exchange model for the nucleon-nucleon interaction, Phys. Rev. C **45**, 2094 (1992)
13. A. Stadler, F. Gross and M. Frank, Covariant equations for the three-body bound state, Phys. Rev. C **56**, 2396 (1997)
14. F. Gross, G. Ramalho and M. T. Peña, Covariant nucleon wave function with  $S$ ,  $D$ , and  $P$ -state components, Phys. Rev. D **85**, 093005 (2012)
15. F. Gross, G. Ramalho and M. T. Peña, Spin and angular momentum in the nucleon, Phys. Rev. D **85**, 093006 (2012)
16. S. Capstick and W. Roberts, Quark models of baryon masses and decays, Prog. Part. Nucl. Phys. **45**, S241 (2000)
17. M. M. Giannini and E. Santopinto, The hypercentral Constituent Quark Model and its application to baryon properties, Chin. J. Phys. **53**, 020301 (2015)
18. G. Ramalho and K. Tsushima, Octet baryon electromagnetic form factors in a relativistic quark model, Phys. Rev. D **84**, 054014 (2011); G. Ramalho and K. Tsushima, Covariant spectator quark model description of the  $\gamma^* \Lambda \rightarrow \Sigma^0$  transition, Phys. Rev. D **86**, 114030 (2012)
19. G. Ramalho, K. Tsushima and A. W. Thomas, Octet Baryon Electromagnetic form Factors in Nuclear Medium, J. Phys. G **40**, 015102 (2013)
20. F. Gross and P. Agbakpe, The Shape of the nucleon, Phys. Rev. C **73**, 015203 (2006)
21. C. Savkli and F. Gross, Quark-antiquark bound states in the relativistic spectator formalism, Phys. Rev. C **63**, 035208 (2001)
22. G. Ramalho and M. T. Peña, Extracting the  $\Omega^-$  electric quadrupole moment from lattice QCD data, Phys. Rev. D **83**, 054011 (2011)
23. G. Ramalho and K. Tsushima, Axial form factors of the octet baryons in a covariant quark model, Phys. Rev. D **94**, 014001 (2016)
24. G. Ramalho, Semirelativistic approximation to the  $\gamma^* N \rightarrow N(1520)$  and  $\gamma^* N \rightarrow N(1535)$  transition form factors, Phys. Rev. D **95**, 054008 (2017)
25. G. Ramalho and M. T. Peña, A covariant model for the  $\gamma N \rightarrow N(1535)$  transition at high momentum transfer, Phys. Rev. D **84**, 033007 (2011)
26. G. Ramalho and M. T. Peña,  $\gamma^* N \rightarrow N^*(1520)$  form factors in the spacelike region, Phys. Rev. D **89**, 094016 (2014)
27. G. Ramalho and M. T. Peña, Nucleon and  $\gamma N \rightarrow \Delta$  lattice form factors in a constituent quark model, J. Phys. G **36**, 115011 (2009)
28. G. Ramalho and M. T. Peña,  $\gamma^* N \rightarrow N^*(1520)$  form factors in the timelike regime, Phys. Rev. D **95**, 014003 (2017)
29. G. Ramalho and M. T. Peña, Timelike  $\gamma^* N \rightarrow \Delta$  form factors and Delta Dalitz decay, Phys. Rev. D **85**, 113014 (2012)
30. G. Ramalho, M. T. Peña, J. Weil, H. van Hees and U. Mosel, Role of the pion electromagnetic form factor in the  $\Delta(1232) \rightarrow \gamma^* N$  timelike transition, Phys. Rev. D **93**, 033004 (2016)
31. G. Ramalho and K. Tsushima, Octet to decuplet electromagnetic transition in a relativistic quark model, Phys. Rev. D **87**, 093011 (2013)
32. G. Ramalho and K. Tsushima, What is the role of the meson cloud in the  $\Sigma^{*0} \rightarrow \gamma \Lambda$  and  $\Sigma^* \rightarrow \gamma \Sigma$  decays?, Phys. Rev. D **88**, 053002 (2013)
33. T. Sato and T. -S. H. Lee, Dynamical Models of the Excitations of Nucleon Resonances, J. Phys. G **36**, 073001 (2009)
34. B. Julia-Diaz, T.-S. H. Lee, T. Sato and L. C. Smith, Extraction and Interpretation of  $\gamma N \rightarrow \Delta$  Form Factors within a Dynamical Model, Phys. Rev. C **75**, 015205 (2007)

35. T. Sato and T. S. H. Lee, Dynamical study of the Delta excitation in  $N(e, e'\pi)$  reactions, Phys. Rev. C **63**, 055201 (2001)
36. S. S. Kamalov and S. N. Yang, Pion cloud and the  $Q^2$  dependence of  $\gamma^*N \leftrightarrow \Delta$  transition form-factors, Phys. Rev. Lett. **83**, 4494 (1999)
37. B. Julia-Diaz, H. Kamano, T. S. H. Lee, A. Matsuyama, T. Sato and N. Suzuki, Dynamical coupled-channels analysis of  $p(e, e'\pi)N$  reactions, Phys. Rev. C **80**, 025207 (2009)
38. G. Ramalho, M. T. Peña and A. Stadler, The shape of the  $\Delta$  baryon in a covariant spectator quark model, Phys. Rev. D **86**, 093022 (2012)
39. G. Ramalho and M. T. Peña, Electromagnetic form factors of the  $\Delta$  in a  $S$ -wave approach, J. Phys. G **36**, 085004 (2009)
40. G. Ramalho, M. T. Peña and F. Gross, Electromagnetic form factors of the  $\Delta$  with  $D$ -waves, Phys. Rev. D **81**, 113011 (2010); G. Ramalho, M. T. Peña and F. Gross, Electric quadrupole and magnetic octupole moments of the  $\Delta$ , Phys. Lett. B **678**, 355 (2009)
41. F. Gross, G. Ramalho and K. Tsushima, Using baryon octet magnetic moments and masses to fix the pion cloud contribution, Phys. Lett. B **690**, 183 (2010)
42. G. Ramalho, D. Jido and K. Tsushima, Valence quark and meson cloud contributions for the  $\gamma^*A \rightarrow A^*$  and  $\gamma^*\Sigma^0 \rightarrow A^*$  reactions, Phys. Rev. D **85**, 093014 (2012)
43. G. Ramalho and K. Tsushima, A Model for the  $\Delta(1600)$  resonance and  $\gamma N \rightarrow \Delta(1600)$  transition, Phys. Rev. D **82**, 073007 (2010)
44. I. G. Aznauryan *et al.* [CLAS Collaboration], Electroexcitation of nucleon resonances from CLAS data on single pion electroproduction, Phys. Rev. C **80**, 055203 (2009)
45. M. M. Dalton *et al.*, Electroproduction of  $\eta$  Mesons in the  $S_{11}(1535)$  Resonance Region at High Momentum Transfer, Phys. Rev. C **80**, 015205 (2009)
46. H. Kamano, Electromagnetic  $N^*$  Transition Form Factors in the ANL-Osaka Dynamical Coupled-Channels Approach, Few Body Syst. **59**, 24 (2018). Contribution to the workshop.
47. V. I. Mokeev *et al.* [CLAS Collaboration], Experimental Study of the  $P_{11}(1440)$  and  $D_{13}(1520)$  resonances from CLAS data on  $ep \rightarrow e'\pi^+\pi^-p'$ , Phys. Rev. C **86**, 035203 (2012)
48. V. I. Mokeev *et al.*, New Results from the Studies of the  $N(1440)1/2^+$ ,  $N(1520)3/2^-$ , and  $\Delta(1620)1/2^-$  Resonances in Exclusive  $ep \rightarrow e'p'\pi^+\pi^-$  Electroproduction with the CLAS Detector, Phys. Rev. C **93**, 025206 (2016)
49. J. Beringer *et al.* [Particle Data Group Collaboration], Review of Particle Physics (RPP), Phys. Rev. D **86**, 010001 (2012)
50. V. D. Burkert,  $N^*$  Experiments and their Impact on Strong QCD Physics, Few Body Syst. **59**, 57 (2018). Contribution to the workshop
51. V. I. Mokeev [CLAS Collaboration], Nucleon Resonance Structure from Exclusive Meson Electroproduction with CLAS, Few Body Syst. **59**, 46 (2018). Contribution to the workshop
52. L. Tiator, Few Body Syst. **59**, no. 3, 21 (2018) Contribution to the workshop.
53. G. Ramalho and K. Tsushima, A simple relation between the  $\gamma N \rightarrow N(1535)$  helicity amplitudes, Phys. Rev. D **84**, 051301 (2011)
54. D. Jido, M. Doering and E. Oset, Transition form factors of the  $N^*(1535)$  as a dynamically generated resonance, Phys. Rev. C **77**, 065207 (2008)
55. G. Ramalho and K. Tsushima, Valence quark contributions for the  $\gamma N \rightarrow P_{11}(1440)$  form factors, Phys. Rev. D **81**, 074020 (2010)
56. G. Ramalho and K. Tsushima,  $\gamma^*N \rightarrow N(1710)$  transition at high momentum transfer, Phys. Rev. D **89**, 073010 (2014)
57. I. G. Aznauryan, Electroexcitation of the Roper resonance in the relativistic quark models, Phys. Rev. C **76**, 025212 (2007)
58. G. Ramalho and K. Tsushima, Valence quark contributions for the  $\gamma N \rightarrow P_{11}(1440)$  transition, AIP Conf. Proc. **1374**, 353 (2011)
59. S. J. Brodsky, G. F. de Teramond, H. G. Dosch and J. Erlich, Light-Front Holographic QCD and Emerging Confinement, Phys. Rept. **584**, 1 (2015)
60. G. Ramalho and D. Melnikov, Valence quark contributions for the  $\gamma^*N \rightarrow N(1440)$  form factors from Light-Front holography, Phys. Rev. D **97**, 034037 (2018)
61. G. Ramalho, Analytic parametrizations of the  $\gamma^*N \rightarrow N(1440)$  form factors inspired by light-front holography, Phys. Rev. D **96**, 054021 (2017)

62. H. F. Jones and M. D. Scadron, Multipole  $\gamma N$ - $\Delta$  form-factors and resonant photoproduction and electroproduction, *Annals Phys.* **81**, 1 (1973)
63. G. Ramalho, Parametrizations of the  $\gamma^* N \rightarrow \Delta(1232)$  quadrupole form factors and Siegert's theorem, *Phys. Rev. D* **94**, 114001 (2016)
64. G. Ramalho, New low- $Q^2$  measurements of the  $\gamma^* N \rightarrow \Delta(1232)$  Coulomb quadrupole form factor, pion cloud parametrizations and Siegert's theorem, *Eur. Phys. J. A* **54**, 75 (2018)
65. G. Ramalho, Combined parametrization of the neutron electric form factor and the  $\gamma^* N \rightarrow \Delta(1232)$  quadrupole form factors, arXiv:1710.10527 [hep-ph]
66. G. Ramalho, Improved empirical parametrizations of the  $\gamma^* N \rightarrow N(1535)$  transition amplitudes and the Siegert's theorem, *Phys. Lett. B* **759**, 126 (2016)
67. C. Becchi and G. Morpurgo, Vanishing of the E2 part of the  $N_{33}^* \rightarrow N + \gamma$  amplitude in the non-relativistic quark model of elementary particles, *Phys. Lett.* **17**, 352 (1965)
68. A. J. Buchmann and E. M. Henley, Intrinsic quadrupole moment of the nucleon, *Phys. Rev. C* **63**, 015202 (2000)
69. C. Alexandrou *et al.*,  $\Delta$ -baryon electromagnetic form factors in lattice QCD, *Phys. Rev. D* **79**, 014507 (2009)
70. V. Pascalutsa, M. Vanderhaeghen and S. N. Yang, Electromagnetic excitation of the  $\Delta(1232)$ -resonance, *Phys. Rept.* **437**, 125 (2007)
71. C. Alexandrou, G. Koutsou, H. Neff, J. W. Negele, W. Schroers and A. Tsapalis, Nucleon to delta electromagnetic transition form factors in lattice QCD, *Phys. Rev. D* **77**, 085012 (2008)
72. C. E. Carlson and N. C. Mukhopadhyay, Approach to perturbative results in the  $N$ - $\Delta$  transition, *Phys. Rev. Lett.* **81**, 2646 (1998); C. E. Carlson, Perturbative QCD applied to baryons, *Few Body Syst. Suppl.* **11**, 10 (1999)
73. P. E. Shanahan, A. W. Thomas, K. Tsushima, R. D. Young and F. Myhrer, Octet Spin Fractions and the Proton Spin Problem, *Phys. Rev. Lett.* **110**, 202001 (2013)
74. F. Dohrmann *et al.*, A versatile method for simulating  $pp \rightarrow ppe^+e^-$  and  $dp \rightarrow pne^+e^- p_{\text{spec}}$  reactions, *Eur. Phys. J. A* **45**, 401 (2010)
75. W. J. Briscoe, M. Döring, H. Haberzettl, D. M. Manley, M. Naruki, I. I. Strakovsky and E. S. Swanson, Physics Opportunities with Meson Beams, *Eur. Phys. J. A* **51**, 129 (2015)
76. J. Weil, H. van Hees, and U. Mosel, Dilepton production in proton-induced reactions at SIS energies with the GiBUU transport model, *Eur. Phys. J. A* **48**, 111 (2012) [Erratum-ibid. A **48**, 150 (2012)]
77. J. Adamczewski-Musch *et al.* [HADES Collaboration],  $\Delta(1232)$  Dalitz decay in proton-proton collisions at  $T = 1.25$  GeV measured with HADES at GSI, *Phys. Rev. C* **95**, 065205 (2017)
78. B. Ramstein, Time-Like Baryon Transitions in Hadroproduction. Contribution to the workshop
79. V. Pascalutsa and M. Vanderhaeghen, Large- $N_c$  relations for the electromagnetic  $N \rightarrow \Delta(1232)$  transition, *Phys. Rev. D* **76**, 111501 (2007)
80. A. J. Buchmann, J. A. Hester and R. F. Lebed, Quadrupole moments of  $N$  and  $\Delta$  in the  $1/N_c$  expansion, *Phys. Rev. D* **66**, 056002 (2002)
81. A. Blomberg *et al.*, Electroexcitation of the  $\Delta^+(1232)$  at low momentum transfer, *Phys. Lett. B* **760**, 267 (2016)
82. N. Sparveris,  $N$  to  $\Delta$  transition: recent results and prospects. Contribution to the workshop
83. A. J. Buchmann, E. Hernandez, U. Meyer and A. Faessler,  $N \rightarrow \Delta(1232)$   $E2$  transition and Siegert's theorem, *Phys. Rev. C* **58**, 2478 (1998)
84. L. Tiator, D. Drechsel, S. S. Kamalov and M. Vanderhaeghen, Electromagnetic Excitation of Nucleon Resonances, *Eur. Phys. J. ST* **198**, 141 (2011)
85. L. Tiator and S. Kamalov, Nucleon resonance excitation with virtual photons, AIP Conf. Proc. **904**, 191 (2007); L. Tiator, Pion Electroproduction and Siegert's Theorem, *Few Body Syst.* **57**, 1087 (2016)
86. G. Ramalho, Improved empirical parametrizations of the  $\gamma^* N \rightarrow \Delta(1232)$  and  $\gamma^* N \rightarrow N(1520)$  helicity amplitudes and the Siegert's theorem, *Phys. Rev. D* **93**, 113012 (2016)
87. V. I. Mokeev, [https://userweb.jlab.org/~mokeev/resonance\\_electrocouplings/](https://userweb.jlab.org/~mokeev/resonance_electrocouplings/)

- 
88. A. J. G. Hey and J. Weyers, Quarks and the helicity structure of photoproduction amplitudes, *Phys. Lett. B* **48**, 69 (1974)
  89. W. N. Cottingham and I. H. Dunbar, Baryon Multipole Moments In The Single Quark Transition Model, *Z. Phys. C* **2**, 41 (1979)
  90. V. D. Burkert, R. De Vita, M. Battaglieri, M. Ripani and V. Mokeev, Single quark transition model analysis of electromagnetic nucleon resonance transitions in the  $[70, 1^-]$  supermultiplet, *Phys. Rev. C* **67**, 035204 (2003)
  91. I. G. Aznauryan, V. D. Burkert, G. V. Fedotov, B. S. Ishkhanov and V. I. Mokeev, Electroexcitation of nucleon resonances at  $Q^2 = 0.65 \text{ (GeV/c)}^2$  from a combined analysis of single- and double-pion electroproduction data, *Phys. Rev. C* **72**, 045201 (2005)
  92. M. Dugger *et al.* [CLAS Collaboration],  $\pi^+$  photoproduction on the proton for photon energies from 0.725 to 2.875 GeV, *Phys. Rev. C* **79**, 065206 (2009)